Phys Chem Minerals (2012) 39:589–598
DOI 10.1007/s00269-012-0514-z

ORIGINAL PAPER

Thermal equation of state of $Mg_3Al_2Si_3O_{12}$ pyrope garnet up to 19 GPa and 1,700 K

Yongtao Zou · Steeve Gréaux · Tetsuo Irifune · Matthew L. Whitaker · Toru Shinmei · Yuji Higo

Received: 13 February 2012 / Accepted: 17 May 2012 / Published online: 8 June 2012

Abstract Thermoelastic properties of synthetic $Mg_3Al_2Si_3O_{12}$ pyrope garnet have been measured at high pressure and high temperature by using in situ energy-dispersive X-ray diffraction, using a Kawai-type multi-anvil apparatus. Measurements have been conducted up to 19 GPa and 1,700 K, equivalent to the *P–T* conditions of the middle part of mantle transition zone. Analyses of the room-temperature *P–V* data to a third-order Birch–Murnaghan (BM) equation of state (EoS) yields: $V_0 = 1{,}500 \pm 1$ Å^3, $K_0 = 167 \pm 6$ GPa and $K_0' = 4.6 \pm 0.3$. When fitting the entire *P–V–T* data using a high-temperature Birch–Murnaghan (HTBM) EoS at a fixed $K_{T0}' = 4.6$, we obtain $V_0 = 1{,}500 \pm 2$ Å^3, $K_{T0} = 167 \pm 3$ GPa, $(\partial K/\partial T)_P = -0.021 \pm 0.009$ GPa K^{-1} and $\alpha_{300} = (2.89 \pm 0.33) \times 10^{-5}$ K^{-1}. Fitting the present data to the Mie-Grüneisen-Debye (MGD) EoS with Debye temperature $\Theta_0 = 806$ K gives $\gamma_0 = 1.19$ and 1.15 at fixed $q = 1.0$ and 1.5, respectively. Comparison of these fittings with two different approaches, we propose to constrain the bulk modulus and its pressure derivative to $K_0 = 167$ GPa and $K_0' = 4.4$–4.6, as well as the Grüneisen parameter to $\gamma_0 = 1.15$–1.19.

Keywords Pyrope garnet · X-ray diffraction · Thermoelastic properties · Static compression · High pressure and high temperature

Y. Zou (✉) · S. Gréaux · T. Irifune · M. L. Whitaker · T. Shinmei
Geodynamics Research Center, Ehime University, Matsuyama 790-8577, Japan
e-mail: yongtaozou@yahoo.com.cn

Y. Zou
Graduate School of Science and Engineering, Ehime University, Matsuyama 790-8577, Japan

Present Address:
M. L. Whitaker
Mineral Physics Institute, Stony Brook University, Stony Brook, NY 11794-2100, USA

Y. Higo
Japan Synchrotron Radiation Institute, Hyogo 679-5198, Japan

Introduction

Silicate garnets are considered important constituents in the Earth's upper mantle and mantle transition zone, comprising 40 % by volume of the pyrolite composition (Irifune and Ringwood 1987). Garnets are also important components of subducted oceanic crust, and it is suggested that garnet-rich subducted crust can be gravitationally trapped in the lowermost part of mantle transition zone (Irifune and Ringwood 1993; Karato et al. 1995). It is well accepted that garnet should play a significant role in the nature and dynamics of the shallow to the middle part of the Earth's mantle. Therefore, understanding the thermoelastic properties of garnets is of great importance in interpreting compositional models and regional seismic profiles of the upper 660 km of the Earth's interior (Duffy and Anderson 1989; Weidner and Wang 2000).

Pyrope garnet with the composition of $Mg_3Al_2Si_3O_{12}$ is the magnesium end-member of garnets group, and therefore, its physical properties are of great significance. Elastic properties of pyrope garnet for both natural single crystals and synthetic polycrystals have been investigated by many scientists with various techniques, including ultrasonic interferometry, Brillouin scattering and static compression methods (Zhang et al. 1998; Leger et al. 1990; Conrad et al. 1999; Chen et al. 1999; Wang and Ji 2001;

Sinogeikin and Bass 2000, 2002; Gwanmesia et al. 2006, 2007). Yagi et al. (1987) measured the *P–V–T* relations of pyrope at high pressure and high temperature in a DIA-type cubic-anvil apparatus, but the experimental pressure was limited to ~6 GPa. Subsequently, static compression experiments of pyrope garnet were performed by Zhang et al. (1998) in a diamond anvil cell (DAC) up to 33 GPa at room temperature. Afterward, Conrad et al. (1999) carried out Brillouin scattering experiments on a natural pyrope garnet at pressures up to 10 GPa and room temperature. However, the reported pressure derivative for bulk modulus $K' = 3.22$ showed a significantly discrepancy, as compared with those of previous studies (Zhang et al. 1998; Leger et al. 1990; Chen et al. 1999; Wang and Ji 2001; Sinogeikin and Bass 2000, 2002; Gwanmesia et al. 2006, 2007). Recently, elasticity of pyrope has been measured up to 9 GPa and 1,000 °C using the ultrasonic interferometric techniques (Gwanmesia et al. 2006), but these experimental *P–T* conditions are not accessible to the mantle conditions. To date, experimental studies on the elastic/thermoelastic properties of pyrope garnet at in situ high *P–T* conditions are still limited. Previous studies were performed either at high temperature and ambient pressure (Sinogeikin and Bass 2002; Gwanmesia et al. 2007) or at high pressure and room temperature (Zhang et al. 1998; Leger et al. 1990; Chen et al. 1999; Conrad et al. 1999; Wang and Ji 2001).

In this study, we have investigated the pressure–volume–temperature (*P–V–T*) relations of synthetic $Mg_3Al_2Si_3O_{12}$ pyrope garnet at *P–T* conditions up to 19 GPa and 1,700 K, equivalent to the middle part of mantle transition region, using a Kawai-type multi-anvil apparatus combined with in situ energy-dispersive X-ray diffraction (EDXRD) at Beamline BL04B1 (SPring-8, Japan). The thermoelastic properties of pyrope garnet are obtained by the fittings of the present *P–V–T* data to the high-temperature Birch–Murnaghan (HTBM) EoS and Mie-Grüneisen-Debye (MGD) formulism, respectively.

Experimental procedures

Starting material for hot-pressed synthesis experiments was glass with $Mg_3Al_2Si_3O_{12}$ composition, prepared by melting a mixture of oxides at 1,873 K in a Pt crucible. Polycrystalline samples of pyrope garnet were synthesized at 12 GPa and 1,200 °C for 1.5 h using a Kawai-type multi-anvil apparatus at Geodynamics Research Center (Ehime University, Japan). X-ray diffraction patterns collected before compression confirmed that the synthetic sample was a single phase of pyrope garnet, as shown in Fig. 1. SEM-EDX analyses further proved that the synthetic sample was a single phase with the composition as follows

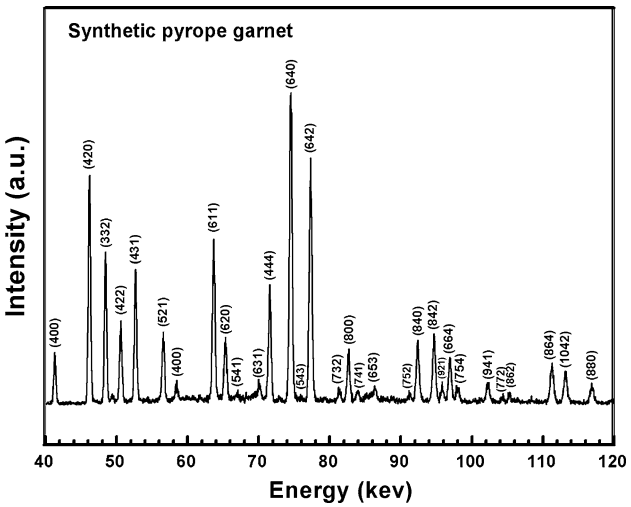

Fig. 1 In situ X-ray diffraction pattern of the synthetic pyrope garnet before compression suggesting that the synthetic sample was a single garnet phase and no other phases were observed

(in wt%): MgO, 29.8(2); Al_2O_3, 24.5(3); SiO_2, 44.5(2), which can be also written in term of formula unit as $Mg_{3.00}Al_{1.99}Si_{3.01}O_{12}$.

High-pressure and high-temperature in situ experiments were performed in a cubic-anvil DIA-type apparatus (SPEED-1500) installed at the synchrotron beamline BL04B1 (SPring-8, Japan). High pressure was generated by so-called 11/5 cell assembly consisted of semi-sintered (Mg, Co)O octahedron pressure medium of 11.0 mm in edge length, in which a Re heater and a $LaCrO_3$ sleeves served as thermal insulators were inserted. Tungsten carbide cubic anvils with 5.0 mm truncation edge length (TEL = 4.0 mm) supported by pyrophyllite gaskets were used as the second-stage anvils of the high-pressure apparatus. An MgO window was placed in $LaCrO_3$ sleeves for obtaining X-ray diffraction path to the sample. The details of this high *P–T* experimental cell assembly can be found elsewhere (i.e. Gréaux et al. 2011; Higo et al. 2008). The cell pressure was determined using the equation of state of gold (pressure marker) as proposed by Tsuchiya (2003). The temperature was measured using $W_{97}Re_3$-$W_{75}Re_{25}$ thermocouple, the hot junction of which was placed near the pressure marker without correction of the effect of pressure on the thermoelectromotive force. In this synchrotron experiment, we have not measured the temperature gradient in this high-pressure cell. However, the temperature difference between the thermocouple junction and the sample/pressure marker was within 1–2 % of the nominal temperatures by two thermocouples in a separate run with a similar cell assemblage, as also suggested by Higo et al. (2008). Moreover, X-ray diffraction patterns were collected within the shortest distance across the interface of the sample and pressure marker so as to ensure

their similar *P–T* conditions. Therefore, the pressure difference between the pressure marker (Au/NaCl) and the sample was assumed to be negligible.

The equation of state of gold, proposed by Tsuchiya (2003), was used to calculate the pressure from the unit-cell volume of Au. The consistency of this pressure scale with the established NaCl scale by Decker (1971) and Brown (1999) was confirmed by Funamori et al. (1996), in which the differences of the pressures based on these two scales (Au and NaCl) were within 0.2–0.4 GPa at temperatures from 1,000 to 1,600 °C and at pressures near 25 GPa. The obtained thermoelastic properties based on two different pressure scales (Au and NaCl) showed significantly agreements within uncertainties. Meanwhile, the calculated pressures in this study derived from Au scale proposed by Tsuchiya (2003) showed good consistency with those from NaCl scale by Brown (1999). Therefore, we used the gold scale as the primary pressure scale in the present analysis.

Figure 2 shows the pressure–temperature (*P–T*) path of the present high-pressure and high-temperature experiments, up to 19 GPa and 1,700 K. In cycle (1), we first compressed the sample up to ~18 GPa and then increased the temperature to 1,100 K. Heating was maintained at 1,100 K for several minutes at fixed ram loads in order to minimize the effect of non-hydrostatic stress that could develop upon cold compression. In each cycle, in situ X-ray diffraction patterns were collected after heating, during cooling down to 300 K, by 200 K steps. Comparison of the sharp diffraction peaks for both the sample and pressure markers after heating with the counterparts before heating suggested that the residual stresses were substantially reduced by this annealing procedure. Subsequently, the pressure was increased to ~12 GPa at room temperature by means of increasing ram loads. This experimental procedure was repeated for cycles (1) → (6) at the *P–T* conditions up to 19 GPa and 1,700 K. For cycle (7), X-ray diffraction data were measured after release of the pressure during cooling. X-ray diffraction patterns for the pyrope sample collected at the present experimental *P–T* conditions showed that no phase transformation and/or other phases were observed throughout these experiments, which was consistent with the stability field of pyrope reported by Hirose et al. (2001).

Peak positions and extraction of lattice parameters of pyrope garnet as well as gold (pressure marker) were refined by reducing full diffraction patterns following the LeBail method (Le Bail et al. 1988) with the multi-phase profile-fitting technique implemented in the *EXPGUI/GSAS* software package (Larson and Von Dreele 2000; Toby 2001). Precisions in unit-cell volumes for both pyrope garnet and gold (pressure marker) were estimated from the LeBail refinement of X-ray diffraction profiles.

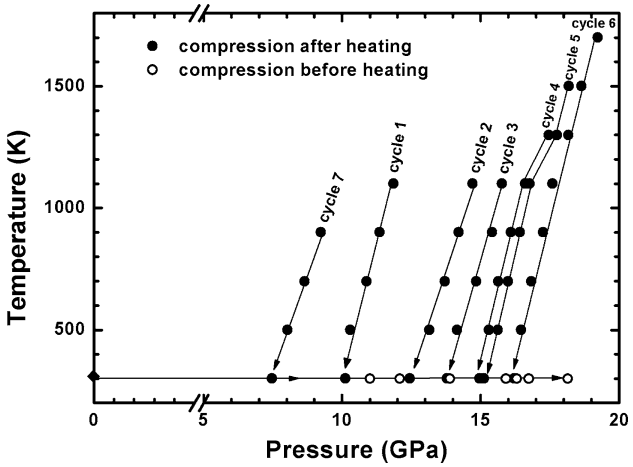

Fig. 2 Experimental *P–T* conditions for energy-dispersive synchrotron X-ray diffraction of $Mg_3Al_2Si_3O_{12}$ pyrope garnet. The *solid circle symbols* represent the pressures after heating, while *open circle symbols* show those before heating. All of the data were collected in the stability field of pyrope garnet reported by Hirose et al. (2001)

Meanwhile, the precision of the pressures calculated by using the equation of state of gold (Tsuchiya 2003) was calculated by taking into account the propagated errors from those of the unit-cell volume of gold.

Results and discussion

Room-temperature equation of state (EoS)

Unit-cell volumes of $Mg_3Al_2Si_3O_{12}$ pyrope garnet obtained along various isotherms from 300 to 1,700 K at pressures up to ~19 GPa are shown in Table 1. X-ray diffraction collected at ambient condition gives the unit-cell volume $V_0 = 1{,}500.43 \pm 0.08$ Å^3. This value is about 0.1 % smaller than the values of $1{,}501.9 \pm 0.1$ Å^3 and 1,501.4 Å^3 reported by Parise et al. (1996) and Sinogeikin and Bass (2000), respectively. Figure 3 shows the room-temperature unit-cell volumes (V) of pyrope garnet as a function of pressure (P). The pressure–volume (*P–V*) relations have been determined by fitting the present room-temperature data to a third-order Birch–Murnaghan equation of state (EoS), which is represented as follows:

$$P = \frac{3}{2}K_0\left[\left(\frac{V_0}{V}\right)^{\frac{7}{3}} - \left(\frac{V_0}{V}\right)^{\frac{5}{3}}\right] \times \left\{1 + \frac{3}{4}\left(K_0' - 4\right)\left[\left(\frac{V_0}{V}\right)^{\frac{2}{3}} - 1\right]\right\} \quad (1)$$

where V_0, K_0 and K_0' are unit-cell volume, isothermal bulk modulus and its pressure derivative at ambient condition, respectively. Analyses of Eq. (1) with all parameters free yield $V_0 = 1{,}500 \pm 1$ Å^3, $K_0 = 167 \pm 6$ GPa and

Table 1 Pressure, temperature, lattice parameter and unit-cell volume of $Mg_3Al_2Si_3O_{12}$ pyrope garnet

P (GPa)	T (K)	a (Å)	V (Å^3)	P (GPa)	T (K)	a (Å)	V (Å^3)
Compression before heating				10.89 (3)	700	11.2704 (3)	1,431.57 (10)
0.00 (2)	300	11.4482 (2)	1,500.43 (8)	13.71 (3)	700	11.2214 (3)	1,412.00 (10)
11.02 (4)	300	11.2282 (2)	1,415.55 (9)	14.84 (3)	700	11.1962 (3)	1,403.48 (11)
18.14 (4)	300	11.1437 (2)	1,383.83 (9)	15.64 (3)	700	11.1850 (3)	1,399.30 (12)
12.08 (3)	300	11.2134 (3)	1,409.99 (10)	15.99 (3)	700	11.1782 (3)	1,396.73 (12)
13.89 (3)	300	11.1878 (3)	1,400.34 (12)	16.83 (4)	700	11.1731 (3)	1,394.84 (11)
15.92 (3)	300	11.1574 (4)	1,388.94 (15)	9.24 (3)	900	11.3190 (3)	1,450.19 (11)
16.30 (3)	300	11.1507 (3)	1,386.44 (13)	11.35 (3)	900	11.2828 (3)	1,436.33 (10)
16.74 (3)	300	11.1394 (4)	1,382.25 (14)	14.20 (2)	900	11.2305 (3)	1,416.45 (11)
Compression after heating				15.41 (3)	900	11.2069 (3)	1,407.51 (11)
7.47 (2)	300	11.2931 (2)	1,440.25 (9)	16.09 (3)	900	11.1955 (3)	1,403.24 (11)
10.12 (2)	300	11.2474 (3)	1,422.83 (10)	16.42 (3)	900	11.1876 (3)	1,400.27 (12)
12.44 (3)	300	11.2075 (3)	1,407.76 (11)	17.26 (4)	900	11.1842 (3)	1,399.00 (10)
13.78 (3)	300	11.1787 (3)	1,396.93 (11)	11.86 (3)	1,100	11.2910 (3)	1,439.46 (10)
14.96 (3)	300	11.1632 (3)	1,391.12 (12)	14.72 (3)	1,100	11.2385 (3)	1,419.48 (10)
15.13 (3)	300	11.1578 (4)	1,389.10 (14)	15.77 (3)	1,100	11.2158 (3)	1,410.89 (11)
16.21 (4)	300	11.1508 (10)	1,386.50 (10)	16.60 (3)	1,100	11.2069 (3)	1,407.54 (11)
8.03 (3)	500	11.3009 (2)	1,443.23 (10)	16.77 (3)	1,100	11.2006 (3)	1,405.16 (12)
10.29 (2)	500	11.2595 (3)	1,427.44 (10)	17.60 (4)	1,100	11.1930 (3)	1,402.28 (11)
13.16 (3)	500	11.2112 (3)	1,409.13 (11)	17.46 (3)	1,300	11.2180 (3)	1,411.70 (12)
14.15 (3)	500	11.1868 (3)	1,399.95 (13)	17.75 (3)	1,300	11.2115 (3)	1,409.26 (12)
15.30 (3)	500	11.1749 (3)	1,395.51 (12)	18.16 (4)	1,300	11.2061 (3)	1,407.23 (12)
15.62 (3)	500	11.1670 (3)	1,392.53 (13)	18.18 (3)	1,500	11.2179 (3)	1,411.69 (12)
16.45 (4)	500	11.1615 (3)	1,390.51 (10)	18.64 (4)	1,500	11.2171 (3)	1,411.36 (13)
8.65 (3)	700	11.3100 (3)	1,446.73 (10)	19.23 (4)	1,700	11.2267 (3)	1,414.98 (12)

Numbers in parenthesis represent the errors calculated for P, a and V

$K_0' = 4.6 \pm 0.3$, which is in good agreement with previous results of $K_0 = 171 \pm 2$ GPa and $K_0' = 4.4 \pm 0.2$ by Zhang et al. (1998) within mutual uncertainties, and also consistent with the sound velocity data of $K_{T0} = 169.4 \pm 1.1$ GPa and $K_{T0}' = 4.55 \pm 0.20$ reported by Gwanmesia et al. (2007). On the other hand, our pressure derivative of $K_0' = 4.6 \pm 0.3$ cannot agree with that of $K_0' = 3.8 \pm 1.0$ proposed by Leger et al. (1990) at a fixed $K_0 = 172.8$ GPa. However, if we fix K_0' to 4.0, fitting of Eq. (1) gives $K_0 = 171 \pm 1$ GPa, which seems comparable to Leger et al.'s (1990) value. In fact, as shown in Fig. 3, it is likely that the scattering in Leger et al.'s (1990) experimental data gives poor constraints on the determination of the pressure derivative for the bulk modulus, resulting in a smaller value $K_0' = 3.8$. Figure 3 shows that the present P–V relations of pyrope garnet agree well with those of Zhang et al. (1998) with increasing pressure up to ~24 GPa. However, with the increase in pressure from 24 to 33 GPa, deviation can be observed significantly between our fitting curve/data at fixed $K_0' = 4.0$ and Zhang et al.'s (1998) data. Meanwhile, the red curve fitted with all the parameters free (i.e. $K_0' = 4.6 \pm 0.3$) is in a good agreement with the data of Zhang et al. (1998), which gives a strong argument for a value of K_0' close to ~4.6. For comparison, we have plotted the previous P–V data points by Gwanmesia et al. (2006), which shows good agreements with the present fitting results in black and red curves with increasing pressure up to ~7 GPa, respectively. Our results suggest that $K_0' < 4.0$ for $K_0 \sim 170$ GPa (fixed), as suggested by previous studies (Leger et al. 1990; Conrad et al. 1999), cannot explain the compression behaviors of pyrope over its entire P–T stability field. Thus, based on the present study, we propose to constrain the bulk modulus and its pressure derivative to $K_0 = 167$ GPa and $K_0' = \sim 4.6$.

P–V–T relations and thermoelastic properties

The pressure–volume–temperature (P–V–T) relations of pyrope garnet were investigated at pressures and

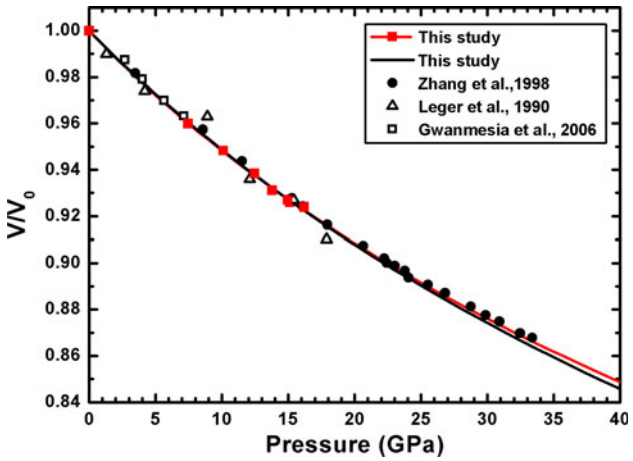

Fig. 3 *P–V* relations of static compression data of $Mg_3Al_2Si_3O_{12}$ pyrope garnet at 300 K obtained in this study, compared with previous studies by Zhang et al. (1998), Leger et al. (1990), and Gwanmesia et al. (2006), respectively. *Solid red squares* symbolize the present data points. The *red curve* shows the fitting results of this study by using the third-order Birch–Murnaghan equation of state, giving $K_0 = 167 \pm 6$ GPa and $K_0' = 4.6 \pm 3$. The *black curve* represents the fitting results of the present study at a fixed K_{T0}' = 4.0, yielding $K_0 = 171 \pm 1$ GPa and $V_0 = 1{,}500 \pm 1$ Å^3. *Solid circles*, *open triangles* and *open squares* are experimental data at room temperature by Zhang et al. (1998), Leger et al. (1990) and Gwanmesia et al. (2006), respectively

temperatures up to ~19 GPa and 1,700 K with two different approaches. The high-temperature Birch–Murnaghan (HTBM) and the Mie-Gruneisen-Debye (MGD) equations of state were used to extract the thermoelastic properties of pyrope garnet. First, we describe the HTBM equation of state, as shown below:

$$P(V,T) = \frac{3}{2}K_{T0}\left[\left(\frac{V_{T0}}{V}\right)^{\frac{7}{3}} - \left(\frac{V_{T0}}{V}\right)^{\frac{5}{3}}\right] \times \left\{1 + \frac{3}{4}\left(K_{T0}' - 4\right)\left[\left(\frac{V_{T0}}{V}\right)^{\frac{2}{3}} - 1\right]\right\} \quad (2)$$

where K_{T0}, K_{T0}' and V_{T0} are the isothermal bulk modulus, its pressure derivative and the unit-cell volume at temperature T and ambient pressure, respectively. In Eq. (2), the pressure derivative K_{T0}' is assumed to be constant throughout the whole temperature range. The thermal dependence of the bulk modulus is expressed by a linear function of temperatures (Eq. 3), assuming that the temperature derivative $(\partial K_T/\partial T)_P$ is constant in the temperature range of this study:

$$K_{T0} = K_0 + \left(\frac{\partial K_T}{\partial T}\right)_P (T - 300) \quad (3)$$

$$K_{T0}' = K_0' \quad (4)$$

where K_0 and K_0' are the bulk modulus and its pressure derivative at ambient P–T condition, respectively. The temperature derivative for the unit-cell volume V_{T0} can be estimated by a function of the thermal expansion at ambient pressure α_T, which has an empirical assumption of $\alpha_T = a_0 + b_0 T$, where a_0 and b_0 are constant parameters:

$$V_{T0} = V_0 \exp \int_{300}^{T} \alpha_T dT. \quad (5)$$

Table 2 lists the parameters of V_0, K_{T0}, K_{T0}', $(\partial K_T/\partial T)_P$, a_0 and b_0 derived from the fitting of our data to the HTBM equation of state. Due to the scattering in these data, fitting all the parameters simultaneously yields a smaller $K_{T0} = 164.1 \pm 9.5$ GPa and a higher $K_{T0}' = 4.95 \pm 1.19$ (e.g. Table 2), compared with the previous studies (Sinogeikin and Bass 2000, 2002; Gwanmesia et al. 2006, 2007; Zhang et al. 1998). In addition, the uncertainties on the elastic parameters are generally large, resulting in a difficult discussion on this fitting. These results suggest that even with the large pressure and temperature range covered in this study, the present data may be not sufficient to constrain all the thermoelastic parameters at the same time during fitting. Therefore, we chose to fix K_{T0}' to 4.6, as suggested by our room-temperature P–V fitting results. Fitting of the present P–V–T data to the HTBM EoS at a fixed $K_{T0}' = 4.6$ yields: $V_0 = 1{,}500 \pm 2$ Å^3, $K_{T0} = 167 \pm 3$ GPa, $(\partial K_T/\partial T)_P = -0.021 \pm 0.009$ GPa K^{-1} and $\alpha_{300} = (2.89 \pm 0.33) \times 10^{-5}$ K^{-1}. This bulk modulus $K_{T0} = 167 \pm 3$ GPa is in good agreement with the previous Brillouin scattering value of 169.4 ± 2.0 GPa by Sinogeikin and Bass (2000), the P–V–T data of 167 ± 4 by Gwanmesia et al. (2006) and the sound velocity data of 169.4 GPa by Gwanmesia et al. (2007) within mutual uncertainties, respectively.

The yielded value of $(\partial K_T/\partial T)_P = -0.021 \pm 0.009$ GPa K^{-1} is almost as same as the previous data within uncertainties (see Table 2; Wang et al. 1998; Sinogeikin and Bass 2000, 2002; Gwanmesia et al. 2006, 2007). As shown in Fig. 4, the temperature dependence of bulk modulus $(\partial K_T/\partial T)_P$ at $K_{T0}' = 4.6$ is in good agreement with the P–V–T data of Gwanmesia et al. (2006). Moreover, our data can well shed light on the previous thermoelastic data reported by Anderson et al. (1991) at high temperatures. It can be seen that the fitted gray and black lines of Wang et al. (1998) and Sinogeikin and Bass (2000) can explain the reported data by Anderson et al. (1991) at temperatures below ~400 K, whereas significant disagreements can be observed at temperatures more than ~400 K, respectively. The same behavior can be observed in the present fittings at $K_{T0}' = 4.1$ (fixed) and 4.95 (constraint-free), suggesting that the temperature dependence of bulk modulus $(\partial K_T/\partial T)_P$ of the fitting at $K_{T0}' = 4.6$ is close to -0.021 ± 0.009 GPa K^{-1}. In addition, we have found that the thermal parameter

Table 2 Thermoelastic parameters derived from the high-temperature Birch–Murnaghan (HTBM) EoS of pyrope garnet, as compared with previous studies

V_0 (Å^3)	K_{T0}	K'_{T0}	$(\partial K_S/\partial T)_P$ or $(\partial K_T/\partial T)_P$ GPa K^{-1}	α_{300} (10^{-5} K^{-1})	a_0 (10^{-5} K^{-1})	b_0 (10^{-8} K^{-2})	References
1,500.7 (19)	164.1 (95)	4.95 (1.2)	−0.024 (13)	2.97 (45)	2.63 (26)	1.14 (64)	This study
1,499.9 (15)	170.7 (30)	4.1[a]	−0.017 (9)	2.74 (33)	2.48 (21)	0.88 (42)	
1,500.4 (15)	166.8 (30)	4.6[a]	−0.021 (9)	2.89 (33)	2.58 (20)	1.02 (46)	
1,500.8 (15)	163.8 (30)	5.0[a]	−0.024 (9)	2.98 (34)	2.64 (19)	1.15 (51)	
1,501.4[b]	169.4 (20)	4.1 (3)	−0.019 (3)	–	–	–	Sinogeikin and Bass (2000, 2002)
1,502.9 (3)	171 (2)	4.4 (2)	–	–	–	–	Zhang et al. (1998)
1,502.5[b]	167 (4)	3.9[a]	−0.022	–	–	–	Gwanmesia et al. (2006)-*P–V–T* data
1,504.4[b]	169.4	4.55 (20)	−0.0206	–	–	–	Gwanmesia et al. (2007)
1,503.1 (5)	170 (2)	5.0[a]	−0.020 (3)	2.58 (28)	2.3 (2)	0.94 (28)	Wang et al. (1998)

[a] Values were fixed during data processing

[b] Values were calculated from the corresponding densities

$(\partial K_T/\partial T)_P$ is almost unaffected by the variations of K'_{T0}, whereas the value of K_{T0} deviate significantly because of the strong correlation between K_{T0} and K'_{T0}(Table 2). The thermal expansivities α_T derived from the fitting at fixed $K'_{T0} = 4.6$ and 4.95 (i.e. no constraint) agree well with that of Wang et al. (1998). Figure 5 shows the pressure–volume–temperature (*P–V–T*) relations of $Mg_3Al_2Si_3O_{12}$ pyrope garnet, in which the thermoelastic parameters determined from this study ($V_0 = 1{,}500 \pm 2$ Å^3, $K_{T0} = 167 \pm 3$ GPa, $K'_{T0} = 4.6$, $\alpha_{300} = (2.89 \pm 0.33) \times 10^{-5}$ K^{-1} and $(\partial K/\partial T)_P = -0.021 \pm 0.009$ GPa K^{-1}) are applied.

The present *P–V–T* data also have been analyzed by using the Mie-Grüneisen-Debye (MGD) equation of state (e.g. Jackson and Rigden 1996). In this model, the pressure is described by the sum of the static pressure at room temperature and the thermal pressure (Eq. 6)

$$P(V,T) = P(V,T_0) + \Delta P\mathrm{th}(V,T) \tag{6}$$

$$\Delta P\mathrm{th}(V,T) = \frac{\gamma(V)}{V}[E\mathrm{th}(V,T) - E\mathrm{th}(V,T_0)] \tag{7}$$

In Eq. 6, the static pressure $P(V,T_0)$ is expressed by a third-order Birch–Murnaghan EoS (Eq. 1), whereas the thermal pressure $\Delta P\mathrm{th}(V,T)$ is described as a function of the Grüneisen parameter γ and the thermal energy $E\mathrm{th}(V,T)$. The thermal energy can be evaluated with a Debye function (Debye 1912), as expressed below:

$$E\mathrm{th}(V,T) = 9nRT\left(\frac{\Theta}{T}\right)^{-3}\int_0^{\frac{\Theta}{T}}\frac{x^3}{e^x-1}dx \tag{8}$$

$$\Theta = \Theta_0 \exp\left(\frac{\gamma_0 - \gamma}{q}\right) \tag{9}$$

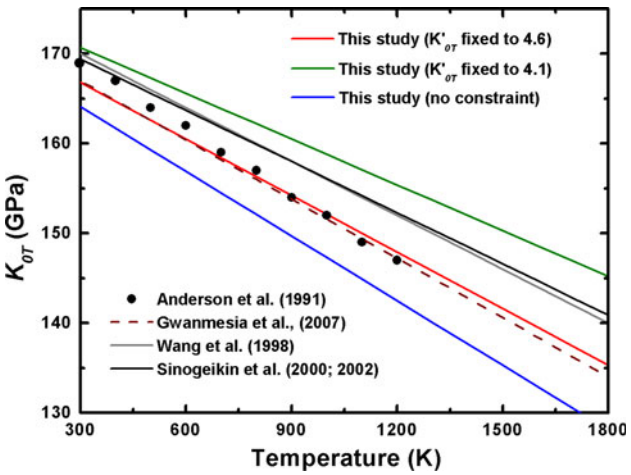

Fig. 4 Isothermal bulk modulus K_{T0} as a function of temperature. *Solid red*, *green* and *blue lines* represent the present results for fixed values of $K'_{T0} = 4.6$ and 4.1, as well as for no constraint on the elastic parameters ($K_{T0} = 164.1$ GPa and $K'_{T0} = 4.95$). *Dash brown*, *solid gray* and *solid black lines* symbolize the previous studies by Gwanmesia et al. (2007), Wang et al. (1998) and Sinogeikin and Bass (2000), respectively. *Solid circles* are experimental values reported by Anderson et al. (1991)

$$\gamma = \gamma_0\left(\frac{V}{V_0}\right)^q \tag{10}$$

where n is the number of atoms per formula unit, R is the gas constant, Θ is the Debye temperature, γ_0 and Θ_0 are the Grüneisen parameter and the Debye temperature at V_0, respectively. The Debye temperature Θ is assumed to be a function of volume and independent of temperature.

In this approach, six parameters V_0, K_{T0}, K'_{T0}, γ_0, Θ_0 and q can be determined by the fitting of the present *P–V–T* data to MGD equation of state. Similar to the fitting using HTBM equation of state, the scattering in the present data

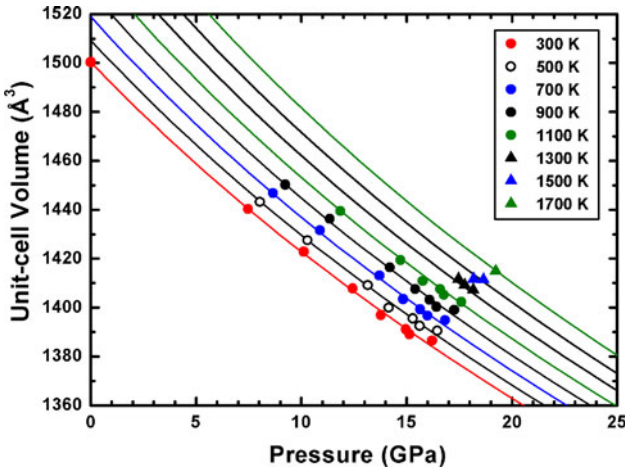

Fig. 5 *P–V–T* relations of pyrope garnet obtained from the present study (*different symbols*). Isothermal compression *curves* at various temperatures (*different color curves*) are calculated by using the yielded thermoelastic parameters of the present study. ($V_0 = 1{,}500 \pm 2$ Å^3, $K_{T0} = 167 \pm 3$ GPa, $K'_{T0} = 4.6$, $(\partial K/\partial T)_P = -0.021 \pm 0.009$ GPa K^{-1} and $\alpha_{300} = (2.89 \pm 0.33) \times 10^{-5}$ K^{-1})

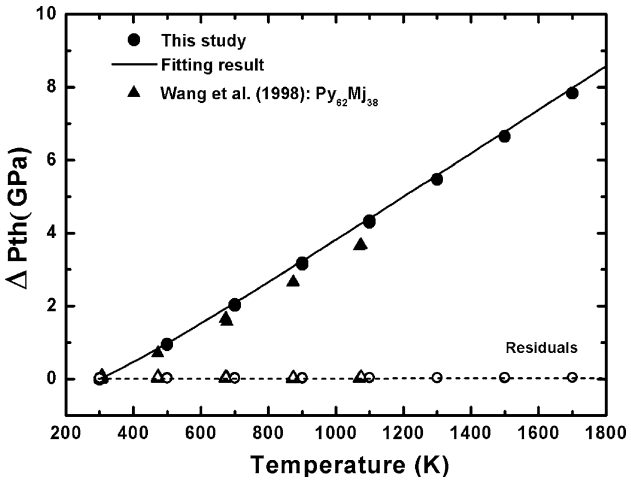

Fig. 6 Thermal pressure ΔP_{th} of pyrope garnet using the Mie-Grüneisen-Debye models as a function of temperature, compared with the previous counterparts of pyrope-majorite ($Py_{62}Mj_{38}$) by Wang et al. (1998). The residuals are represented with *open symbols* of the same shape as the corresponding experimental data

makes it difficult to constrain the parameters up to 6 at the same time during the fitting by MGD equation of state. For a wide range of materials, the volume dependence of γ is shown to hold with $q \approx 1$ (Stixrude and Bukowinski 1990), and therefore, most of the previous fittings have been carried out with q fixed at values of 0.5–1.5 for minerals (e.g., Duffy and Ahrens 1995; Jackson and Rigden 1996). For example, Gréaux et al. (2011) have pointed out that unit-cell volume and bulk modulus of grossular garnet, which is an analog to pyrope garnet, are unaffected, when q values vary from 0 to 1.4.

Therefore, for ease of comparison, the values $q = 1$ and $\Theta_0 = 806$ K are determined to be fixed during this fitting, where the Debye temperature $\Theta_0 = 806$ K is calculated based on the previous sound velocity measurements data by Sinogeikin and Bass (2000, 2002; $V_P = 9.12$ km/s, $V_S = 5.13$ km/s, $\rho = 3.57$ g/cm^3 at ambient condition). When fitting the present *P–V–T* data to MGD equation of state at fixed $q = 1$ and $\Theta_0 = 806$ K, we obtain $V_0 = 1{,}502$ Å^3, $K_{T0} = 167$ GPa, $K'_{T0} = 4.44$ and $\gamma_0 = 1.19$ (RMS misfit on the pressure $\sim$0.09 GPa). The present Grüneisen parameter $\gamma_0 = 1.19$ is generally in good agreement with the value of $\gamma_0 = 1.17$ proposed by Wang et al. (1998), in which an assumption of the Debye temperature $\Theta_0 = 790$ K is applied. When fitting at $q = 0.5$ and $\Theta_0 = 806$ K, we obtain the values of $\gamma_0 = 1.31$ and $K'_{T0} = 4.46$. It is also found that the unit-cell volume and bulk modulus at ambient condition are almost unaffected by changes in q values during fittings. Fitting the present *P–V–T* data to MGD equation of state at $q = 1.5$ and $\Theta_0 = 806$ K gives $K'_{T0} = 4.44$ and $\gamma_0 = 1.15$, which is slightly smaller than the value $\gamma_0 = 1.19$ determined from the fitting at $q = 1.0$ and $\Theta_0 = 806$ K. It can be seen that the yielded values of $\gamma_0 = 1.15$–1.19 ($q = 1$–1.5) are in good agreement with the value of $\gamma_0 = 1.11$ ($q = 0.8$) reported by recent ab Initio molecular dynamic simulation (Li et al. 2011).

Figure 6 shows thermal pressure ΔPth of pyrope together with that of majorite-pyrope garnet against temperature, suggesting that the thermal pressure depends essentially on the temperature, with almost negligible effects on the volume changes as well as an obvious compositional dependence. Therefore, on the basis of the present results, we propose to constrain the thermoelastic parameters of q and γ_0 for pyrope garnet to 1.0–1.5 and 1.15–1.19, respectively.

Figure 7 shows selected X-ray diffraction patterns (one run) of the pyrope garnet sample under various *P–T* conditions. It can be seen that the relative intensity of the peaks for pyrope garnet are almost unchanged with increasing pressures and temperatures up to 19.23 GPa and 1,700 K, except for a slightly weak intensity of (611) peak for pyrope garnet, compared with that of (642) peak at the highest *P–T* conditions. Transmission electron microscopy (TEM) shows that the synthetic pyrope sample is well-sintered and equilibrium textures formed without secondary phases. TEM imaging of the recovered sample shows an average grain size of about 2–3 μm, whereas the grain size of the synthetic pyrope sample is about 1–2 μm, indicating that grain growth in pyrope garnet is significantly modest after high *P–T* treatments. Moreover, fine grains do not show observable crystal preferred orientation, which is usually observed in large grained counterparts. Therefore, we assume that the effect of the texture

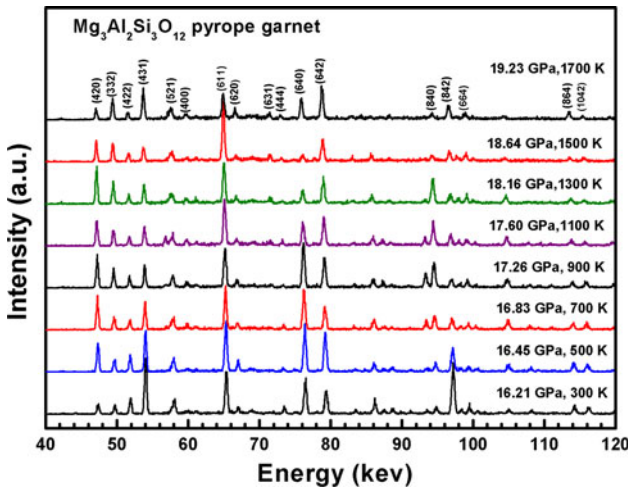

Fig. 7 Selected in situ X-ray diffraction patterns for $Mg_3Al_2Si_3O_{12}$ pyrope garnet at various pressure and temperature conditions

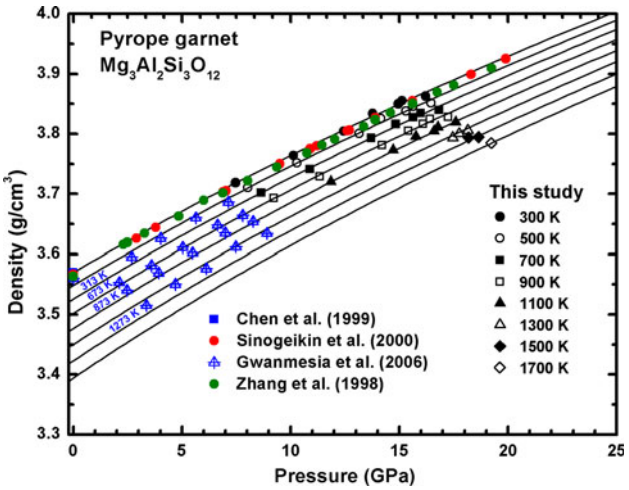

Fig. 8 X-ray density changes for $Mg_3Al_2Si_3O_{12}$ pyrope garnet as a function of pressure and temperature determined from in situ X-ray diffraction measurements. The *solid curves* show the fitting results of the present study using the obtained thermoelastic parameters ($V_0 = 1{,}500 \pm 2$ Å^3, $K_{T0} = 167 \pm 3$ GPa, $K'_{T0} = 4.6$, $(\partial K/\partial T)_P = -0.021 \pm 0.009$ GPa K^{-1} and $\alpha_{300} = (2.89 \pm 0.33) \times 10^{-5}$ K^{-1}), yielding a zero-pressure density of 3.569(1) g/cm^3. *Blue squares*, *red circles*, *blue cross triangles* and *green circles* symbolize the previous studies by Chen et al. (1999), Sinogeikin and Bass (2000), Gwanmesia et al. (2006) and Zhang et al. (1998), respectively

development on the lattice parameters at in situ high *P–T* conditions remains negligible.

Figure 8 shows the density changes for $Mg_3Al_2Si_3O_{12}$ pyrope garnet with pressure and temperature obtained from the present measurements, yielding a zero-pressure density of 3.569(1) g/cm^3, which is in good agreement with the earlier ultrasonic measurement result of 3.57(2) g/cm^3 by Chen et al. (1999). Moreover, the present densities at 300 K are in good agreement with the previous Brillouin scattering data by Sinogeikin and Bass (2000) and static compression data by Zhang et al. (1998) within the experimental uncertainties, respectively. In contrast, the present densities are slightly larger than those from the recent ultrasonic measurement data by Gwanmesia et al. (2006), which may be due to the larger unit-cell volume of 1,502.5 Å^3 at ambient condition, as compared with the present value of 1,500 Å^3.

The present study describes EoS models from two different approaches, which gives significantly consistent thermoelastic parameters. From these data, we are able to constrain the bulk modulus and its pressure derivative to $K_{T0} = 167$ GPa and $K'_{T0} = 4.5$–4.6, as well as the Grüneisen parameter to $\gamma_0 = 1.15$–1.19. Throughout the present experiment, we have not observed phase decomposition and/or phase transformation from cubic to tetragonal garnet as observed in majorite garnet (Heinemann et al. 1997). The composition and crystal structure of natural garnets at high *P–T* conditions can be complex, and therefore, it is important to constrain elastic parameters of pure end members from self-consistent data over a large range of *P–T* conditions presented in this work. Indeed, our data do not provide sufficient constraints for seismic data interpretation, but these data can be used to estimate accurately the densities of pyrope garnet at the high *P–T* conditions up to the mantle transition zone (i.e. see Fig. 8).

Conclusions

Experimental study of the high-pressure behavior of silicate garnets is of great importance to constrain the compositional dependence of thermoelastic properties of those minerals/mantle materials. Such results are particularly valuable for the understanding the elastic properties of natural garnets at high *P–T* conditions, because they usually appear with relatively complex compositions.

The pressure–volume–temperature (*P–V–T*) measurements have been carried out on pyrope garnet up to 19 GPa and 1,700 K. Using the high-temperature Birch–Murnaghan (HTBM) and Mie-Grüneisen-Debye (MGD) equations of state/formulism, we have obtained the thermoelastic properties of pyrope garnet at pressures and temperatures close to the mantle conditions. These thermoelastic properties determined from two different approaches show good agreements with each other. The analyses of the present *P–V–T* data to the HTBM EoS give $V_0 = 1{,}500 \pm 2$ Å^3, $K_{T0} = 167 \pm 3$ GPa, $(\partial K_T/\partial T)_P = -0.021 \pm 0.009$ GPa K^{-1} and $\alpha_{300} = (2.89 \pm 0.33) \times 10^{-5}$ K^{-1} with a fixed $K'_{T0} = 4.6$. Fitting of the present data to the MGD EoS at $\Theta_0 = 806$ K and $q = 1.0$ yields $V_0 = 1{,}502$ Å^3,

$K_{T0} = 167$ GPa, $K'_{T0} = 4.4$ and $\gamma_0 = 1.19$ (RMS misfi ~ 0.09 GPa). When fitting with fixed values of $q = 0.5$ and 1.5 at $\Theta_0 = 806$ K, we obtain the values of $\gamma_0 = 1.31$ and 1.15, respectively, whereas V_0, K_0 and K'_{T0}remain almost unchanged. On the basis of this study, we propose to constrain the bulk modulus and its pressure derivative to $K_0 = 167$ GPa and $K'_{T0} = 4.4$–4.6, as well as the Grüneisen parameter to $\gamma_0 = 1.15$–1.19. These new thermoelastic parameters can well explain the various data obtained previously by different methods over a large *P–T* range and therefore have provided stronger convincing evidence to solve the previous disagreements on the thermoelastic properties of $Mg_3Al_2Si_3O_{12}$ pyrope garnet.

Acknowledgments The authors thank Y. Tange, N. Nishiyama and R. Negishi for their assistance in this experiment on BL04B1 at SPring-8 (Proposal No. 2011A0082). We are grateful to F. Wang, C. Zhou and C. Yang for valuable discussion. We also acknowledge two anonymous reviewers for their valuable comments, which improved the manuscript, and C. McCammon for editorial handling. This research was supported by the Global-COE program "Deep Earth Mineralogy".

References

Anderson OL, Isaak DL, Oda H (1991) Thermoelastic parameters for six minerals at high temperature. J Geophys Res 96:18037–18046

Brown JM (1999) The NaCl pressure standard. J Appl Phys 86:5801–5808

Chen G, Cooke JA, Gwanmesia GD, Liebermann RC (1999) Elastic wave velocities of $Mg_3Al_2Si_3O_{12}$-pyrope garnet to10 GPa. Am Mineral 84:384–388

Conrad PG, Zha CS, Mao HK, Hemley RJ (1999) The high-pressure, single-crystal elasticity of pyrope, grossular, and andradite. Am Mineral 84:374–383

Debye P (1912) The theory of specific warmth. Ann Phys 39:789–839

Decker DL (1971) High-pressure equation of state for NaCl, KCl, and CsCl. J Appl Phys 42:3239–3244

Duffy TS, Ahrens TJ (1995) Compressional sound velocity, equation of state, and constitutive response of shock-compressed magnesium oxide. J Geophys Res 100:529–542

Duffy TS, Anderson DL (1989) Seismic velocity in mantle minerals and mineralogy of the upper mantle. J Geophys Res 94:1895–1912

Funamori N, Yagi T, Utsumi W, Kondo T, Uchida T, Seki M (1996) Thermoelastic properties of $MgSiO_3$ perovskite determined by in situ X ray observations up to 30 GPa and 2000 K. J Geophys Res 101:8257–8270

Gréaux S, Kono Y, Nishiyama N, Kunimoto T, Wada K, Irifune T (2011) *P-V-T* equation of state of $Ca_3Al_2Si_3O_{12}$ grossular garnet. Phys Chem Miner 38:85–94

Gwanmesia GD, Zhang J, Darling K, Kung J, Li B, Wang L, Neuville D, Liebermann RC (2006) Elasticity of polycrystalline pyrope $Mg_3Al_2Si_3O_{12}$) to 9 GPa and 1,000 °C. Phys Earth Planet Inter 155:179–190

Gwanmesia GD, Jackson I, Liebermann RC (2007) In search of the mixed derivative $\partial^2 M/\partial P \partial T$ ($M = G$, K): joint analysis of ultrasonic data for polycrystalline pyrope from gas- and solid-medium apparatus. Phys Chem Miner 34:85–93

Heinemann S, Sharp TG, Seifert F, Rubie DC (1997) The cubic-tetragonal phase transition in the system majorite ($Mg_4Si_4O_{12}$)-pyrope ($Mg_3Al_2Si_3O_{12}$), and garnet symmetry in the Earth's transition zone. Phys Chem Miner 24:206–221

Higo Y, Inoue T, Irifune T, Funakoshi K, Li B (2008) Elastic wave velocities of $(Mg_{0.91}Fe_{0.09})_2SiO_4$ ringwoodite under *P–T* conditions of the mantle transition region. Phys Earth Planet Inter 166:67–174

Hirose K, Fei Y, Ono S, Yagi T, Funakoshi K (2001) In situ measurements of the phase transition boundary in $Mg_3Al_2Si_3O_{12}$: implications for the nature of the seismic discontinuities in the Earth's mantle. Earth Planet Sci Lett 184:567–573

Irifune T, Ringwood AE (1987) Phase transformation in primitive MORB and Pyrolite compositions to 25 GPa and some geophysical implications. In: Manghnani MH, Syono Y (eds) High pressure research in mineral physics, vol 39. TERRA-PUB Tokyo/American Geophysical Union, Washington, DC, pp 235–246

Irifune T, Ringwood AE (1993) Phase transformation in subducted oceanic crust and buoyancy relationships at depths of 600–800 km in the mantle. Earth Planet Sci Lett 117:101–110

Jackson I, Rigden SM (1996) Analysis of *P-V-T* data: constraints on the thermoelastic properties of high-pressure minerals. Phys Earth Planet Int 96:85–112

Karato S, Wang Z, Liu B, Fujino K (1995) Plastic deformation of garnets: systematics and implications for the rheology of the mantle transition zone. Earth Planet Sci Lett 130:13–30

Larson AC, Von Dreele RB (2000) GSAS general structure analysis system operation manual. Los Alamos Natl Lab LAUR 86–748:1–179

Le Bail A, Duroy H, Fourquet JL (1988) Ab initio structure determination of $LiSbWO_6$ by X-ray powder diffraction. Mater Res Bull 23:447–452

Leger JM, Redon AM, Chateau C (1990) Compressions of synthetic pyrope, spessartine and uvarovite garnets up to 25 GPa. Phys Chem Miner 17:161–167

Li L, Weidner DJ, Brodholt J, Alfè D, Price GD (2011) Ab initio molecular dynamic simulation on the elasticity of $Mg_3Al_2Si_3O_{12}$ pyrope. J Earth Sci 22:169–175

Parise JB, Wang Y, Gwanmesia GD, Zhang J, Sinelnikov Y, Chmielowski J, Weidner DJ, Liebermann RC (1996) The symmetry of garnets on the pyrope ($Mg_3A1_2Si_3O_{12}$)-majorite ($MgSiO_3$) join. Geophys Res Lett 23:3782–3799

Sinogeikin SV, Bass JD (2000) Single-crystal elasticity of pyrope and MgO to 20 GPa by Brillouin scattering in the diamond cell. Phys Earth Planet Inter 120:43–62

Sinogeikin SV, Bass JD (2002) Elasticity of pyrope and majorite-pyrope solid solutions to high temperatures. Earth Planet Sci Lett 203:549–555

Stixrude L, Bukowinski MST (1990) Fundamental thermodynamic relations and silicate melting with implications for the constitution of D'. J Geophys Res 95:19311–19325

Toby BH (2001) EXPGUI, a graphical user interface for GSAS. J Appl Cryst 34:210–213

Tsuchiya T (2003) First-principles prediction of the *P-V-T* equation of state of gold and the 660-km discontinuity in Earth's mantle. J Geophys Res 108:2462–2470

Wang Z, Ji S (2001) Elasticity of six polycrystalline silicate garnets at pressure up to 3.0 GPa. Am Mineral 86:1209–1218

Wang Y, Weidner DJ, Zhang J, Gwanrnesia GD, Liebermann RC, Bass JD (1998) Thermal equation of state of garnets along the pyrope-majorite join. Phys Earth Planet Inter 105:59–71

Weidner DJ, Wang Y (2000) Phase transformations: implications for mantle structure, in earth's deep interior: mineral physics and tomography from the atomic to the global scale. In: Karato S et al (eds) Geophys Monogr Ser, vol 117, AGU, Washington, DC, pp 215–235

Yagi T, Akaogi M, Shimomura O, Tamai H, Akimoto S (1987) High pressure and high temperature equations of state of majorite. In: Manghnani MH, Sono Y (eds) High pressure research in mineral physics. Terrapub, Tokyo, pp 141–147

Zhang L, Ahsbahs H, Kutoglu A (1998) Hydrostatic compression and crystal structure of pyrope to 33 GPa. Phys Chem Miner 25:301–307